Journal of Archaeological Science: Reports 8 (2016) 11–14

Contents lists available at ScienceDirect

Journal of Archaeological Science: Reports

journal homepage: www.elsevier.com/locate/jasrep

Fragmentation in zooarchaeological assemblages: The role of equifinal, random processes

Nimrod Marom

Laboratory of Archaeozoology, Zinman Institute of Archaeology, University of Haifa, Mount Carmel, Haifa 3498838, Israel

ARTICLE INFO

Article history:
Received 9 May 2016
Accepted 20 May 2016
Available online xxxx

Keywords:
Zooarchaeology
Fragmentation

ABSTRACT

Bone fragment-size distributions from three archaeological sites were examined in relation to a general model of mechanical fragmentation. The results show a close fit between archaeological bone size distributions and the model for all sites and skeletal elements, regardless of bone marrow content, shape, and recovery/recording procedures. The results suggest that the role played by general equifinal fragmentation processes in archaeological bone assemblage formation may be important, and deserves further study.

1. Introduction

Bone fragmentation intensity is a basic zooarchaeological variable related to in-situ attrition (Stiner, 2002), human butchery (Outram, 2001), assemblage taphonomic history (Lyman 2008: 251–254) and taxonomic composition (Yeshurun et al., 2007). It is usually quantified as the ratio between the number of identified specimens (NISP) and the minimum number of elements (MNE) for a given element and taxon (Grayson and Frey, 2004; Klein and Cruz-Uribe, 1984). The resulting index can be employed, for example, in a correlation analysis with marrow or grease indices in order to infer human butchery intensity (Bar-Oz and Munro, 2007). This fragmentation index, however, may be supplemented by the distribution of individual fragment sizes.

It is argued here that the fragment size distribution could contain important taphonomic information (cf. Hallam, 1967; Trewin and Welsh, 1972) if it can be related to general processes of dynamic fragmentation (Elek and Jaramaz, 2008). An expected distribution of fragment sizes obtained from a generalized random dynamic fragmentation process may tell us how much human-induced variability in fragmentation intensity actually exists between bone elements in our zooarchaeological data. In some cases, we may find that fragment size distribution fits a generalized model of dynamic fragmentation so well that little space is left for human-induced variability in the data, with consequences to taphonomic interpretation.

This study therefore considers the issue of bone fragmentation intensity using the distribution of direct size measurements of identified archaeological bone specimens, in order to examine its fit to a general model of random dynamic fragmentation. In extensively-fragmented bone assemblages there are few large bone fragments and many smaller ones; stricter recovery procedures enhance this pattern (Watson, 1972). I suggest to account for this pattern using a general, random fragmentation process, regardless of the element from which it was originally derived. This should create fragment size distribution with a mean fragment size that reflects the probability of breakage.

This pattern is expected to occur in different bone elements independently of marrow content. In other words, the expected fit of fragment sizes to a simple abundance distribution sees bone as a material undergoing a generalized dynamic fragmentation process, and not as a dietary resource with variable nutrient content; randomised fragmentation, as opposed to cultural patterning, is therefore treated here as the null hypothesis. Since there is an obvious correlation between bone morphology, mechanical susceptibility to breakage and marrow content, the scapula, astragalus and pelvis – possessing different morphology but containing little or no marrow – would be a case in point. If their fragment size distribution shapes cluster with that of marrow yielding long bones, equifinal processes of random dynamic fragmentation can be argued to have affected both marrow-yielding (generally cylindrical) and marrow-poor (and morphologically variable) elements.

I am aware that bone fragmentation is a far more complex process than the simple one described above (Lyman, 2008). The chance of fragmentation events to occur changes in *time* and also as a function of fragment *length*: fragmentation rates decrease after burial and beyond a certain size breakage (or our ability to identify fragments; Marshall and Pilgram, 1991) would cease. The fit of fragment size distribution to a simplified process as the kind described above can be defended both by its parsimony and by the contingency of differential rates of fragmentation on site taphonomic history. The latter would make a more sophisticated model unwieldly at best or otherwise misleading given the diversity of assemblage taphonomic histories.

2. Methods

Bone fragment size distribution data were obtained for identified bones of caprine/caprine-sized ungulates from three Israeli

http://dx.doi.org/10.1016/j.jasrep.2016.05.044
2352-409X/

Table 1
Description of the sampling procedures employed in this study.

Assemblage	Period	Recovery	Recording	Number of measured fragments
Shaar Hagolan	Neolithic (6th millennium BCE)	Dry sieving, 5 mm	All identifiable bone fragments; lengths	526
Mishmar HaEmeq	Neolithic, 9th millennium BCE	Dry sieving, 5 mm	Diagnostic zones; weights	145
Abel Beth Maacha	Bronze–Iron Age, late 2nd millennium BCE	Hand collection	Diagnostic zones; weights	566

Table 2
Statistical data for measured fragments of medium-sized mammals from Sha'ar Hagolan, Stratum E-4. P = proximal, D = distal, PS = proximal shaft, MS = mid-shaft, DS = distal shaft, zone numbers follow Dobney and Rielly (1988). Fragmentation index = NISP/MNE; values in **bold** = above median. Marrow index for sheep from Binford, 1981. The fit of fragment length to the CDF is $R^2 = 0.99$ for all elements. Data in Supplement 1.

	Descriptive statistics (length)					$CDF(x) = 1/(1+e^{-s[x-x']})$					Fragmentation Index	Marrow Index
Element	N	Min	Max	Mean	StDev	x′	s	NISP	MNE	Region?		
Humerus	100	25	105	44.01	13.56	41.15	0.14	125	40	DS	**3.13**	34.9
Radius	51	22	92	47.18	14.30	44.55	0.13	64	17	MS	**3.76**	52.19
Femur	56	22	85	45.29	13.59	43.05	0.13	88	21	MS	**4.19**	47.33
Tibia	67	20	120	50.45	17.68	45.89	0.14	82	18	D	**4.56**	20.76
Metacarpus	17	25	82	45.29	15.83	41.36	0.13	22	8	P	2.75	67.34
Metatarsus	17	30	84	54.76	17.91	52.77	0.08	31	7	PS	**4.43**	68.84
Pelvis	25	22	98	45.64	17.99	41.79	0.11	34	14	Zone 2	2.43	9.75
Scapula	44	18	79	44.93	15.38	42.28	0.11	67	23	Zone 4	2.91	6.23
Vertebrae	69	12	57	35.25	9.40	33.29	0.18	78	22	Zone 1/2	**3.55**	1
Astragalus	16	26	34	30.06	2.29	28.59	0.71	16	15	Zones 1/2/3/4	1.07	1
Calcaneus	20	24	57	39.50	9.89	37.92	0.16	22	19	Zone 2	1.16	23.11
Phalanx 1	44	15	45	32.82	6.51	31.82	0.26	55	48	Zone 2	1.15	33.77

assemblages: (*1*) Neolithic Shaar Hagolan (SHG, Stratum E-4; Garfinkel et al., 2012); (*2*) Neolithic Mishmar HaEmeq (MH; Barzilai and Getzov, 2008); and (*3*) Bronze/Iron Age Abel Beth Maacha (Panitz-Cohen et al., 2013). These assemblages were recovered and recorded in different ways (summarized in Table 1), which is not expected to change the derived fragment size distribution since intra-assemblage consistency in data collection and analysis were maintained. The absence of published individual fragment size data in the literature and the limited availability of assemblages of sufficient size at my disposal does not support a comprehensive analysis that would ideally include more archaeological sites and taxonomic groups.

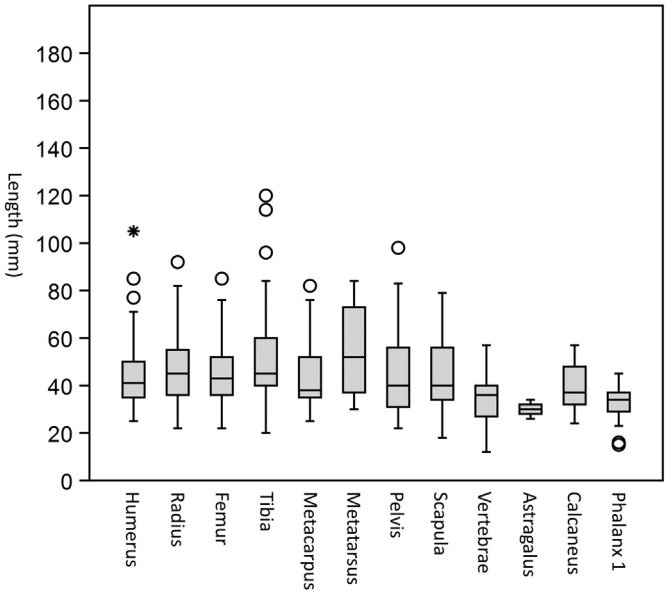

Fig. 1. Fragment lengths of medium-sized mammals in Shaar Hagolan Stratum E-4 plotted by element. The black horizontal line in each box represents the mean; the shaded box and whiskers represent one and two standard deviations, respectively; empty circles represent outliers.

All bone specimens identified to skeletal element and as medium-sized ungulates from SHG were measured lengthwise to the nearest millimetre using Vernier callipers, unless they showed recent (excavation) breakage. The lengths of all specimens were compiled by element, sorted from the largest to the smallest, and plotted as a rank-abundance plot in Microsoft Excel. The size data were binned, transformed to cumulative distribution function (CDF) and fitted to a sigmoid function in Mathematica™. Additionally, MNE values for each element were calculated based on the percentages of completeness of the proximal/distal articulations and the proximal/medial/distal shafts of long bones. The MNE for other elements was derived using the detailed diagnostic zones system of Dobney and Rielly (1988). The fragmentation index for each element was calculated as the NISP/MNE ratio for each element, and correlation between the intensity of fragmentation and a marrow index (Binford, 1981) was sought.

In MH, bones were collected by sieving all the sediments through a 5 mm mesh, as in SHG; however, the faunal analysis employed a focused protocol (based on Davis, 1992) and fragment size was estimated by weight (in grams). In ABM, bones were collected by hand, but were otherwise recorded as at MH. Fragment size distribution in both MH and ABM was analysed as at SHG; however, the focused protocol employed at these sites does not support the calculation of a fragmentation index, since, when using diagnostic zones, NISP = MNE (for methodological discussion see Marom and Bar-Oz, 2008; Trentacoste, 2009).

3. Results

3.1. Fragmentation index

The NISP/MNE index at SHG is not correlated with bone marrow content (Spearman's $R = 0.39$, $P = 0.21$; Table 2). However, five out of six marrow-rich elements (in **bold**, Table 2) show a higher than median value of fragmentation index, whereas the situation is reversed for marrow poor elements (Chi-squared = 5.33; Permutation $P = 0.02$). This result suggests that marrow yielding long bones were more